Structures and properties of phosphate-based bioactive glasses from computer simulation

Jamieson K. Christie,[a] Richard I. Ainsworth,[b], Sergio Ruiz-Hernandez[c] and Nora H. de Leeuw [c]

Phosphate-based bioactive glasses (PBGs) dissolve harmlessly in the body with a dissolution rate which depends sensitively on composition. This makes them proposed vectors for e.g. drug delivery, or other applications where an active component needs to be delivered at a therapeutically appropriate rate. Molecular dynamics (MD) simulations provide atomic-level structural information about PBG compositions. We review recent work to show that MD is an excellent tool to unravel the connec-tions between the PBG glass composition, its atomic structure, and its dissolution rate, which can help to optimise PBGs for specific medical applications.

1 Introduction

Phosphate-based bioactive glasses (PBGs) are solid materials with an amorphous atomic struc-ture containing the PO_4 moiety. Phosphate glasses themselves are useful in several fields, such as optics and nuclear waste encapsulation but our particular interest is in the bioactive com-positions used in biomedical applications. PBGs are especially suited for use as biomaterials be-cause they dissolve harmlessly in the body over a timescale that can vary by several orders of magnitude and which depends sensitively on the glass composition[1]. PBGs can also be synthesised containing therapeutically useful substances[2–4], which are released into the body as the glass dissolves, allowing the use of these glasses in bone repair[4,5], neural repair[6], and the controlled release of antimicrobials[7] or drugs[8]. Amorphous materials are particularly advantageous because their lack of a crystal lattice means that their compositions are not restricted to specific stoichiometries, and hence their properties can be tuned by continuous variations in composition.

In order to understand how the dissolution of these glasses can be optimised for specific medical treatments, we need to have a full understanding of how the dissolution depends on the glass composition and its atomic structure, and how they are affected by the inclusion of dopants (in the form of therapeutic atoms or molecules). It is also important to understand the details of the chemical reactions which occur when the glass is immersed into the physiological environ-ment, for which we need to know the glass struc-

[a] *Department of Materials, Loughborough University, Loughborough, LE11 3TU, UK.*

[b] *Department of Chemistry and Biochemistry, University of California San Diego, 9500 Gilman Drive 0332, La Jolla 92093, California, USA.*

[c;] *School of Chemistry, Cardiff University, Main Building, Park Place, Cardiff, CF10 3AT, UK. Tel.: +44 (0)29 2087 0689. Email: deleeuwn@cardiff.ac.uk*

ture at the surface, and how this changes from that of the bulk.

In the past few years, our groups and oth-ers have extensively used state-of-the-art high-performance computing methods, usually molecular dynamics (MD) simulations, to characterise the structure and properties of PBGs. In molecular dynamics, the individual atoms move due to the interatomic forces they experience from other atoms. Because the full three-dimensional structure of the material is available at all times, an MD trajectory contains a great deal of information from which the material's properties may be deduced. Our work has involved new methodological developments in the form of a new model of the phosphate interatomic forces[9], and MD simulations have given new insight into the structural motifs which affect the dissolution which are not accessible to experimental methods[10]. Recently, the different properties of PBG at the surface of the glass, from where the dissolution takes place have been shown, which will also be important in unravelling the full connections between structure and dissolution[11].

2 Molecular dynamics methods for prepara-tion of glasses

A full review of molecular dynamics methods is beyond the scope of this paper; the reader is invited to turn to relevant books[12,13]. Broadly, there are two types of molecular dynamics used to prepare realistic glass models: classical and first-principles. In classical MD, the interatomic forces are represented by an empirical expression with a small number of parameters which are chosen to reproduce existing data on the material. This method has the advantage of being relatively easy to implement and computation-ally inexpensive, allowing for large models (typ-ically 10^3 10^4 atoms) to be simulated over long timescales (typically ns). The disadvantage is that the accuracy of the simulation is limited by the accuracy of the approximations of the interatomic potential model. First-principles MD, by contrast, uses a quantum-mechanical expression for the interatomic forces which takes account of the material's electronic structure. It is much more accurate, but also much more computation-ally expensive, and models are limited to 10^2 atoms simulated for tens or hundreds of ps.

In both cases, the glass models are prepared using the same "melt and quench" approach with which they would be prepared in the lab. Atoms of the appropriate composition and density are put quasi-randomly into a periodic box which is then equilibrated at a high temperature, typically 2500 K for phosphate glasses, that is well above the melting point to give a properly equilibrated liquid. Equilibration is checked by calculating total and mean-square atomic displacement. The simulated model is then cooled, usually in a series of steps at reducing temperatures, before being equilibrated at room temperature, to provide a disordered solid state. The cooling rate is several orders of magnitude faster than those used experimentally: typical classical MD cooling rates are 1 10 K/ps, and those used in first-principles MD typically vary between 5 100 K/ps. The full effects of the cooling rate on glass properties are not well understood, but the *structure* of the glass is close to experiment for cooling rates slower than 10 K/ps[14–16].

3 Ternary phosphate-based glasses

3.1 Bioactive compositions

Biomedically relevant PBG compositions are ternary in nature, comprising P_2O_5, CaO and Na_2O. The composition of bio-applicable PBGs typically ranges from 45-55 mol% P_2O_5, and so encompasses ultraphosphate, metaphosphate and polyphosphate glass compositions. Compo-sitions containing higher phosphate content lead to more acidic conditions in solution due to in-creased release of HPO_4 and PO^3_4 species, which

eventually lead to bio-incompatibility[17].

3.2 Early first-principles simulations

Tang *et al.*[18] were the first to conduct a simulation of these ternary PBG compositions. They employed first-principles Car-Parinello molecular dynamics (CPMD) to perform a full melt-quench simulation of the ultraphosphate compositions $(P_2O_5)_{0:45}(CaO)_x(Na_2O)_{0:55\ x}$ (x = 0.30, 0.35, and 0.40). The authors analysed the short- and medium-range structure of the glasses at 300 K. Their results showed two well-defined peaks in the P-O radial distribution functions (RDFs) for the three compositions at 1.52 Å and 1.64 Å representing phosphorus atoms covalently bonded to non-bridging oxygens (P-NBO) and bridging oxygens (P-BO) respectively, in good agreement with experimental values[19]. The only dependence on composition for this interaction was a very slight increase in P-BO bond lengths with increasing Ca^{2+}/Na^{+} molar ratio. P-P bond distances and three-body P-O-P bond angles exhibited a strong composition-dependent behaviour, with the full-width-half-maximum (FWHM) val-ues of the respective radial and angular distri-bution functions (ADFs) reducing with increased Ca^{2+}/Na^{+} ratio, suggesting an increased rigidity in the glass network. Despite the limited size of the modelled systems, the medium-range Q^n distributions were analysed and found to contain predominantly a mixture of Q^1 and Q^2 phosphorus, with overall network connectivity values of 1.8 for all three compositions, in agreement with experimental ^{31}P NMR analysis[17].

3.3 Development of an interatomic forcefield for phosphate glass

To overcome the poor statistical sampling offered by the necessarily small periodic unit cells and short simulation times of first-principles simulations, classical methodologies offer an alternative. Prior to 2012, classical molecular dynamics (MD) simulations of phosphate glasses had been limited to binary systems using rigid-ion potentials[20,21], in which the atoms are modelled by point charges. Another study combined x-ray and neutron diffraction along with modelling, via a reverse Monte Carlo simulation, to probe the short-range structure of $(P_2O_5)_{0:50}(CaO)_{0:50}$ [22].

For modelling of bioactive silicate and phosphosilicate glasses, extensive use has been made of polarizable shell-model (SM) forcefields[23]; including the polarizability of the oxygen an-ion leads to much more accurate medium-range structures and Q^n distributions[24]. It is crucial to represent the structure at this length scale correctly to have a full understanding of the link to bioactivity. To extend this approach to phosphate glasses, Ainsworth *et al.*[9] developed a formal-charge polarizable forcefield suitable for multicomponent PBG and conducted melt-quench MD simulations of the compositional range $(P_2O_5)_{0:45}(CaO)_x(Na_2O)_{0:55\ x}$ (x = 0.30, 0.35, and 0.40). The potential was developed by fitting Buckingham-type two-body (P-O) and harmonic three-body (O-P-O and P-O-P) terms to experimental structural and first-principles mechanical data[25] for the o^0(P$_2$O$_5$)¥ crystalline phase. The force field was derived to be compatible with the widely used O-O potential derived by Sanders *et al.*[26] and previously parameterized Ca-O and Na-O potentials for phosphosilicate glasses[27] to give a high-quality formal-charge forcefield for MD simulations of PBG. One challenge in using the SM methodology is constraining the dynamics of the shells at high temperatures, and so a frictional damping term was introduced to prevent non-physical forces being introduced to the simulation.

As with the first-principles MD results of Tang *et al.*,[18] a twin peak P-O RDF was calculated with peaks at 1.49 Å for P-NBO bonds and 1.62 for P-BO bonds for the $(P_2O_5)_{0:45}(CaO)_{0:30}(Na_2O)_{0:25}$ composition (Figure 1), in good agreement with

high energy XRD for the same composition at 1:52 0:02 Å and 1:60 0:02 Å respectively.[19] Small increases and decreases in the P-NBO and P-BO bond lengths respectively were noted for an increasing Ca^{2+}/Na^{+} ratio, due to the relatively higher field strength of Ca^{2+} draw-ing electron density into the bond between modifier and non-bonded oxygen. This fea-ture is also noted in the metaphosphate com-positions $(P_2O_5)_{0:50}(CaO)_x(Na_2O)_{0:50\ x}$ (x=0.00, 0.40, and 0.50) as probed by neutron diffraction and ^{31}P NMR.[28] P coordination, in both simula-tion and experiment, is always very close to four.

The bonding environments of the modifier ions were analysed and showed strong ADF peaks at 77^{o} q 84^{o} indicative of a pseudo-octahedral coordination shell. The authors further decom-posed the coordination environment of the mod-ifier ions into bonds between bridging and non-bridging oxygens. It was shown that the ratio of coordination to NBO versus coordination to BO is greater for calcium than for sodium and that the bonds to NBO are significantly stronger than those to BO (as indicated by the respective bond lengths). Finally, the Q^{n} species distribu-tion showed a proportion of Q^{1} ranging between 26% 29% and Q^{2} between 65% 70% with small amounts of Q^{3}. A minor reversal in the trend of increasing Q^{2} with increasing Ca^{2+}/Na^{+} ratio, as noted in experiment,[19] was also found in the sim-ulated results.

Sodium and calcium enter these glasses as network-modifiying cations, with typical Na-O and Ca-O bond lengths of 2:3 2:4Å, and a pseudo-octahedral first coordination shell. The overall coordination numbers are about 6.5-6.6 for Na and 6.8-6.9 for Ca. Modifier cations typi-cally bond to non-bridging oxygen atoms, but dif-fer in the extent to which they are able to attract the NBOs. For example, in these compositions, the first coordination shell of Na typically had 1.3 BO atoms, with the rest being NBO, whilst Ca had 0.6 BO atoms, with the remainder being NBO.

Di Tommaso *et al.*[16] have also simulated the compositions $(P_2O_5)_{0:45}(CaO)_x(Na_2O)_{0:55\ x}$ (x = 0.30, 0.35, and 0.40) via first-principles and clas-sical MD methodologies in order to focus on the structural and dynamical differences between the liquid melt and the final amorphous glass.

Peak intensities for all RDFs were observed to be lower (by a factor of 1:5 3) in the 3000 K melts than for the final 300 K glasses along with a corresponding increase in the FWHM values reflecting increased thermal motion and struc-tural disorder in the melt. At high temperatures, there was a single P-O peak in the RDF which splits into the two P-BO and P-NBO peaks at 600 K. Increases in calcium content are thought to "decrease(s) the flexibility of the coordina-tion shell of Ca and consequently increase(s) the rigidity of the glass".[16] This is suggested in the FWHM of the P-P RDF reducing from 0.3 Å in $(P_2O_5)_{0:45}(CaO)_{0:30}(Na_2O)_{0:25}$ to 0.12 Å in$(P_2O_5)_{0:45}(CaO)_{0:40}(Na_2O)_{0:15}$. Further, as pre-viously noted by Tang *et al.*,[18] the FWHM of the P-O-P ADF reduces between these compositions, reflecting the effect of Ca^{2+} to increase the rigid-ity of the glass network. Sodium's higher flexi-bility is also clear from the O-Na-O and O-Ca-O ADFs, in which the O-Na-O bond-angle distribu-tion is broader than the O-Ca-O bond-angle dis-tribution.

Medium-range structure was in broad agree-ment with previous theoretical studies. The 3000 K melts had lower amounts of Q^{2} and higher Q^{1} species than the 300 K glasses. The intercon-version of Q^{n} during the melt-quench procedure showed a gradual decrease in Q^{0}, Q^{1} and Q^{3} with a concomitant increase in Q^{2} upon cooling. Inter-estingly for AIMD results the Q^{n} distribution was fully converged at 1500 K whereas for the classi-cal MD melt-quench the distribution converged at 900 K (see Figure 2). As found by Tilocca for silicate glasses,[24] the shell-model potential

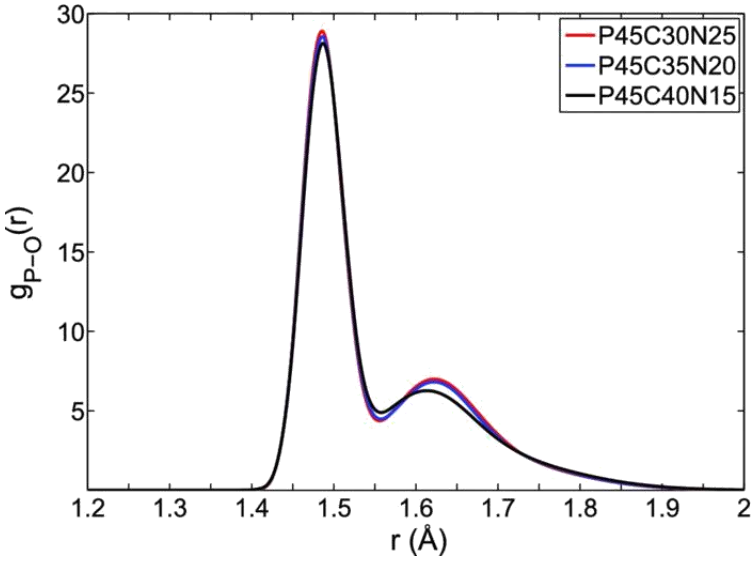

Fig. 1 The simulated P-O radial distribution function, from ref.[9]

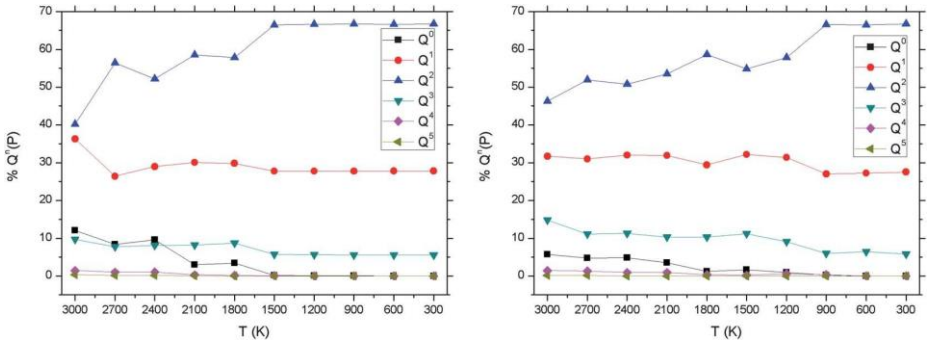

Fig. 2 Interconversion of Q^n species for $(P_2O_5)_{0:45}(CaO)_{0:40}(Na_2O)_{0:15}$ during AIMD (left) and classical MD (right) melt-quenches, from ref.[16]

outperforms non-polarizable potentials by accurately reproducing the difference between P-NBO and P-BO bond lengths, and appropriate Q^n dis-tributions.

From these simulations[9,16,18], and previous experiments[19], the structure of biomedically rele-vant ternary PBG compositions was clear. PO_4 tetrahedra exist in a disordered network broken up by network-modifying Na^+ and Ca^{2+} cations. These phosphate tetrahedra are typically Q^1 or Q^2, that is, connected to one or two other PO_4 tetrahedra, and this connectivity depends only slightly on any changes in the Ca^{2+}/Na^+ ratio. This network connectvity is often cited as a key parameter to explain the dissolution of bioactive glasses[29,30], but here the dissolution changes a great deal at (roughly) constant connectivity. As such, there was still no understanding of what structural motifs could affect dissolution. The key experimental observation linking composi-tion to durability is that increasing the Ca^{2+}/Na^+ ratio leads to a decrease in the glass dissolution rate over orders of magnitude[1].

It seems that the field strength of the network-

modifying cations could be an important parameter. First defined by Dietzel, it is equal to the ionic charge divided by the square of the bond length. This parameter is very strongly corre-lated with the number of bridging oxygen atoms in the first coordination shell of an atom. If two or more cations are present in a glass structure, then they "compete" for the non-bridging oxygen atoms, with the high-field-strength cations win-ning more of them, meaning that the low-field-strength cations coordinate to more BOs.

3.4 Phosphate chains and dissolution rate

Christie *et al.*[10] introduced a new protocol to characterize the environment of the modifier ions, namely by computing the number of unique phosphate chains chemically bound to modifier ions in the glass structure (Figure 3). As men-tioned above, phosphorus atoms in these glasses are mostly Q^1 and Q^2, which means that the over-all network structure is composed of finite-length chains of phosphate tetrahedra. By direct compu-tation, it was found that Ca^{2+} bonds to 3:9 4:0 phosphate chains on average while Na^+ bonds to 3:2 3:3 chains across all the compositions mod-elled. Thus, by increasing the Ca^{2+}/Na^+ ratio the glass network is substantially strengthened.

This effect is also seen in the observation, as discussed above, that Na^+ bonds to more BO than Ca^{2+} in its first coordination shell, which by definition gives two phosphate tetrahedra in the same chain, hence reducing the physical space for more chains to enter the coordination sphere. Christie *et al.*[10] explicitly found that Ca^{2+} has less intra-tetrahedral bonding than Na^+, i.e., two oxygen atoms from the same PO_4 tetrahedron in the first coordination shell, which is also seen in sodium's broader bond-angle distribution, thus contributing to the higher number of unique PO^3_4 tetrahedra that are found around Ca^{2+}. Fi-nally, the average number of $(O\text{-}P\text{-})_n\text{-}O$ chains of length n = 1, 2 and 3 were computed for both Ca^{2+} and Na^+. It was found that shorter chains were more numerous than longer chains around both modifiers and the differences between com-positions were negligible.

That the bonding between phosphate chains and modifier atoms should affect the dissolution is also found through NMR analysis of the species dissolved from PBGs[31]. The glasses dissolve con-gruently, with compositions consisting of phos-phate chains dissolving by the hydration of entire phosphate chains into solution, with any signifi-cant hydrolysis of P-O-P bonds only taking place later. The fact that the phosphate chains do not break up in the glass is consistent with our re-sults that it is the bonding between the whole chain and the modifier which is most important for dissolution.

4 Phosphate-based glasses containing therapeutic ions

Many possible ions have been used or proposed for use with PBGs as a delivery mechanism[32]. These include, among others: silver[7], which is antibiotic; titanium[33], which promotes new bone growth; fluorine[34], which helps prevent dental caries; strontium[35], which is taken up into new bone as a treatment for osteoporosis; and cis-platin[8], which is a chemotherapy drug. The inclusion of therapeutic dopants will of course change the structure of the glass and conse-quently affect its dissolution. Computer simula-tion is able to identify the effects of the additional ingredients on the structure of PBG and interpret the consequences on the dissolution rate. Where classical MD is used, interatomic potentials had to be chosen or developed based on their con-sistency with the pre-existing phosphate poten-tials[9].

4.1 Fluorine

Christie *et al.* used first-principles MD to simu-late fluorinated phosphate glass (F-PBG)[34]. Part

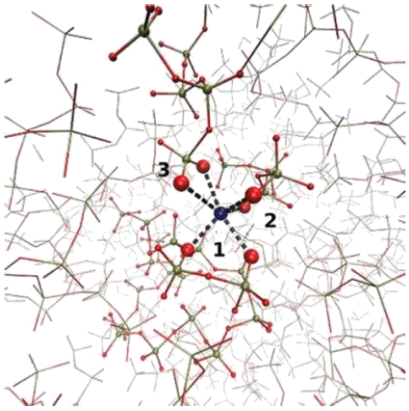

Fig. 3 A Na atom bound to three phosphate chains. Reprinted from ref.[10].

of the motivation for these simulations was to see if F-PBG exhibit the same increased structural heterogeneity that is found in fluorinated bioac-tive silicate glasses[36]. In silicate glass, the fluo-ride ions bond mainly to the network-modifying cations, causing spatial segregation of the glass network into modifier-rich (hence silicate-poor) and modifier-poor (silicate-rich) regions, causing an undesirable variation in bioactivity across the whole sample.

Because of the computational expense of first-principles MD simulations, the number of fluo-rine atoms in the F-PBG simulations was neces-sarily very small, so there are large errors in the structural parameters obtained from these simu-lations. However, the main conclusion was clear: that the F-P coordination number, estimated to be between 0.5 and 0.75, is roughly the same as the F-Ca coordination number (0.5-0.8) and F-Na co-ordination number (0.75-1.5). This implies that there is little or no preferential bonding around the fluoride ions, and that there will be very little mesoscale segregation of the glass structure.

There is no change in the basic structure of the network, of disordered phosphate chains held to-gether by bonding to Na and Ca as modifiers. It might therefore be possible to use fluorinated PBGs as biomedical implants for dental appli-cation as they combine the benefical anticario-genic properties of fluorine with the controlled and tunable dissolution rate of PBGs. These simulations also showed that fluorine inclusion will cause some reduction in network connec-tivity, and hence an increase in the dissolution rate, due to non-bridging fluorine atoms replac-ing bridging oxygen atoms in the coordination shell of phosphorus. However, the overall effect of this is small (a typical P-F coordination num-ber is less than 0.1 for compositions with up to 6 mol% CaF_2) and could be offset by a further small change in the phosphate content.

4.2 Silver

The effect of silver inclusion on PBG structure and dissolution is covered in two works[37,38]. The first of these reports simulation results of metaphosphate (50 mol % P_2O_5) glass compo-sitions, in which Na_2O (sodium field strength = 0.19 e/Å^2) and Ag_2O (with a very similar field strength) are substituted for one another to maintain network connectivity. Silver enters these phosphate glasses as a network modifier, with a typical coordination number of 5.4-5.7, a little smaller than sodium and calcium, which are typically in the range of 6.0-7.0. Like all network-modifying cations, its first coordination shell con-tains mostly non-bridging oxygen (NBO) atoms, with 0.8-1.0 bridging oxygen (BO) atoms. This amount of BO atoms is in between the numbers of BO atoms bonded to Ca (0.5-0.7) and Na (1.0-

1.4).

In terms of the number of phosphate chains to which the different cations are bonded, silver and sodium are rather similar for 45 mol% P_2O_5 content glasses: silver is on average bonded to 3.1 different phosphate chains compared to 3.3 for sodium. It is known experimentally that in-creasing silver content decreases the dissolution rate, rather than the increase which would be expected from weakening the modifier to phos-phate bonding.

4.3 Strontium

Strontium is widely used as a treatment for osteoporosis, one of the symptoms for which is a reduction in bone density. Strontium, like calcium, is taken up into the bone, and can occupy what are normally the calcium sites within the hydroxyapatite bone mineral structure. Recent work[39] suggests that strontium, despite having a larger coordination number than either sodium or calcium, bonds to about the same number of phosphate chains as calcium does, and hence that SrO $ CaO substitution should not affect the dis-solution rate of the glass.

4.4 Bulk structure

Since substantial work has been done on the simulation of PBGs, we have a good understanding of how their *bulk* structure changes, and how this is connected to their dissolution. The network connectivity is often used as a single-parameter measure of how a glass will dissolve, but even from its first introduction, it was clear that it could not explain all features of the connections between glass structure and dissolution[29,30].

As shown in Table 1, if two or more cations exist in the glass, then they compete for the non-bridging oxygen atoms, with the high-field-strength cations winning more of them, mean-ing that the low-field-strength cations have more BOs. This does not mean that the field strength of the network-modifying cation is perfectly correlated to the number of phosphate chains, or the dissolution rate.

Ion	field strength	CN (to NBO)	no. chains
Ag	0.19	5.5 (0.9)	3.1
Na	0.19	6.5 (1.2)	3.3
Ca	0.33	6.8 (0.6)	3.9
Sr	0.28	7.6 (0.9)	4.0

Table 1 The field strength, total coordination number (CN)and coordination number to non-bridging oxygen atoms, and number of phosphate chains bonded to different network-modifying cations.

The number of BO in the first coordination shell is inversely correlated to the field strength (Table 1). The BO/NBO ratio around a given cation affects the number of phosphate chains bonded to it, but exactly how is not clear. Because BO connect two phosphate tetrahedra which will be part of the same chain by definition, an increasing number of BO presumably leads to fewer phosphate chains simply because there is less space around the cation to fit them in.

However, each cation has a different atomic size, bond length, and total coordination number. An increasing total coordination number would allow for more phosphate chains to be bonded to the central cation, simply because n oxygen atoms can come from at most n separate phosphate chains, so a larger value of n could lead to more chains, so the NBO/BO ratio cannot be the only important parameter.

Christie *et al.*[38] also list clustering of network-modifying cations and spatial heterogeneities of the glass network, such as discussed above for fluorine, as features which can affect the disso-lution. Disentangling all of these is rather chal-lenging.

The sol-gel method can be used to prepare phosphate glass containing therapeutic ions[4].

The sol-gel method leaves water inside the bulk glass, which can dissociate and break up the glass network in ways which affect the net-work connectivity and hence bioactivity. No computational work has been done on water-containing phosphate glass so far; *ab initio* MD simulations have been used to study the struc-ture of water in bioactive silicate glass[40], but the use of classical MD for water inside silicate glass has required further development of inter-atomic potential models[41], to include reactive force fields[42,43], the development of which has not begun for phosphate glass.

We know that the dissolution of a phosphate glass proceeds from its surface, and the surface of a material can have quite a different struc-ture and properties to the bulk. In the next sec-tion, we discuss computational methods for un-derstanding the surface structure of PBGs and their link to dissolution.

5 Surfaces

In recent work[11] we have investigated all the dif-ferent surface features that could be involved in the dissolution process of the ternary PBG com-positions. Surfaces were prepared by starting from the volume-optimized bulk supercell, creat-ing two slab geometries with 3D periodicity, but with the top and bottom faces exposed to vac-uum, by elongating the c vector of the simula-tion cell by 30 Å, thus producing surface samples by exposing different sections of the bulk glass. Compositions studied contained 45 mol% P_2O_5, with the rest being Na_2O and CaO; the composi-tions are referred to as, e.g., N25, for the compo-sition with 25 mol% Na_2O.

5.1 Species distribution in the surfaces

All the atoms within 10 Å from the interface were considered to be surface species, in agreement with previous definitions[44]. Significant reorder-ing of the species at the interface occurred in all three glass compositions, including the emer-gence of structural features not usually seen in the bulk. Figures 4 and 5 show example to-pographies observed during the simulation, in-cluding some under-coordinated phosphate units (P3C) (Figure 4), and the formation of multiple-ring structures, some of them formed by three (3M) or four (4M) phosphate units (Figures 4 and 5). Small 3M rings have been found be-fore in experiment[45] and have been reported to be a very significant factor in the nucleation of apatite on silicate-based bioglass[46–48]. Many of the ring structures observed here are directly ex-posed at the interface and disconnected from the main phosphate network.

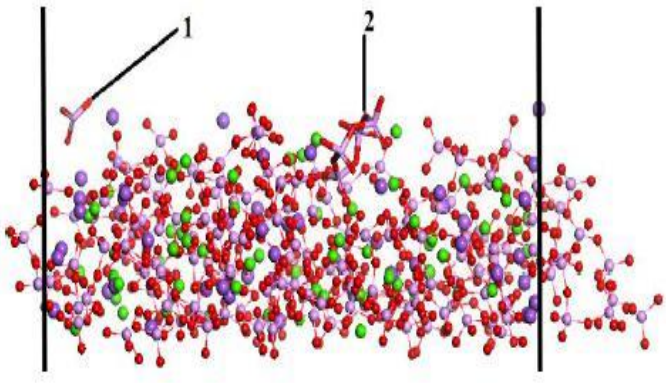

Fig. 4 Side view of a sample surface in N15 showing some features observed after relaxation. Only the top 10 Å of the slab are displayed. (a) Under-coordinated phosphorus (P3c). (b) 4M rings. Colour code: P (pink), O (red), Ca (green) and Na (violet).

The distribution of the species near the in-terface was represented using the proportion of atom x (where x=Ca, Na, O, P), that can be found at height z of the surface (z-profiles) shown in Figure 6, for the three glass concen-trations studied in this work. The interface was defined, rather arbitrarily, as the plane passing through the centre of the topmost oxygen atoms. All surfaces experienced an increase in sodium

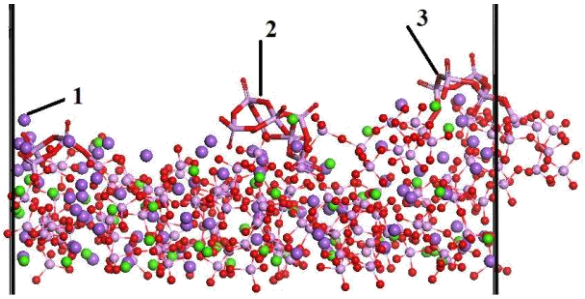

Fig. 5 Side view of a sample surface in N25 showing some features observed after relaxation. Only the top 10 Å of the slab are displayed. (1) Na^+ are the top most cations at the interface (2) 3M ring (3) 4M ring. Colour code: P (pink), O (red), Ca (green) and Na (violet).

concentration over the bulk. In some cases the Na^+ were found as the topmost species in the surface, similar to what has been reported for the silicate-based glasses[49]. In the case of N15 at z > 10 Å, the fraction of sodium equaled the cal-cium value in surfaces with less sodium content. Table 2 confirms that Na^+ is occupying more sur-face sites than Ca^{2+} in N25 and N20, whereas in N15, where the bulk composition of Ca^{2+} is higher than Na^+, the latter only becomes more prominent close to the interface.

The creation of the surfaces also caused the ex-posure of many non-bridging oxygens, several of them projecting out of the interface. The three glass surfaces, which contain similar amounts of oxygen, express higher fractions of NBOs in the top layer compared to the bulk-like region (Ta-ble 2). However, the behaviour of the three glass compositions is slightly different in the layers near the interface. N25 exhibited a minor drop in NBOs compared to the bulk, before attaining

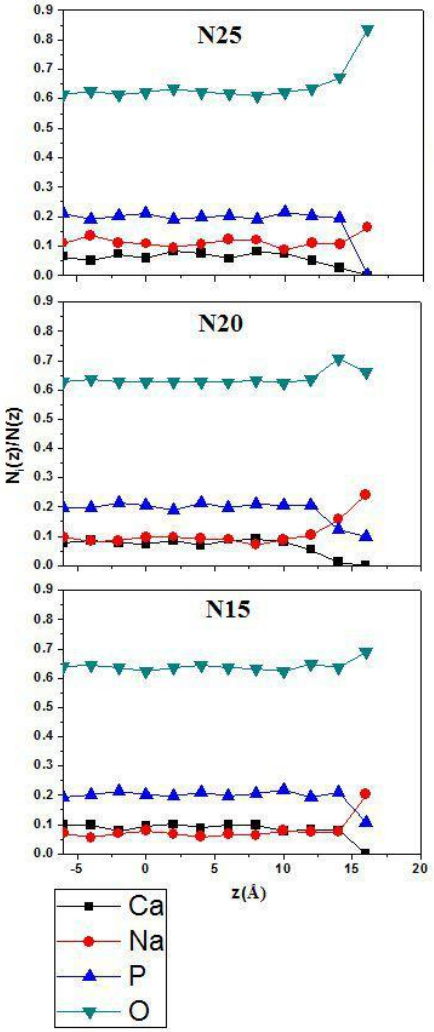

Fig. 6 z-profiles of the fraction of Ca, Na, P and O atoms in the surface slab models after the simulation. Each slab was divided in 2 Å thick slices and the number of atoms in the slice averaged over the MD and further averaged over the four surfaces. z=0 marks the bulk-like region of the slad. From ref.[11]

	Na^+	Ca^{2+}	NBO
N25	2.15	2.21	13.05
N20	1.84	0.78	7.98
N15	2.29	0.83	9.43

Table 2 Concentration (number density nm^{3}) of the different species in the top two layers of the slab.

System	Q^0	Q^1	Q^2	Q^3	NC
N25	0.5	38.8	55.6	5.2	1.65
N20	0.8	40.8	53.4	5.0	1.63
N15	0.5	40.3	52.8	6.4	1.65

Table 3 Q^n distribution (%) calculated for the surface region of the slab in comparison with the bulk. The values are averaged over all surfaces.

the maximum, while N20 showed an increase of NBOs for all z>10 Å[11].

5.2 Surface network

The Q^n distributions for the surfaces (using only the top 10 Å of the slab) of the three glasses are shown in Table 3. For all three compositions, at surface level the phosphorus atoms prefer to have two bridging oxygen atoms, which is similar be-haviour to that observed in the bulk in both theo-retical and experimental studies[9,16]. There is an evident increase in Q^1 and decrease in Q^2 with re-spect to previous calculations of the bulk[9], which is partially due to the surface fracture, but is also strongly linked to the composition of the cation modifiers, which are known to alter the phos-phate network[9,10,16,38]. The same trends were observed in the surfaces and bulk, i.e. an in-crease in Q^1 and decrease in Q^2 with the increase in Ca^{2+} content in the glass (N25 to N20), as re-ported in theoretical studies of the bulk glass[9,16], but there is a small drop in Q^1 from N20 to N15, in agreement with experimental findings in the bulk glasses[9,17].

Another distinctive feature in the surfaces is the increase in Q^0 due to the presence of non-connected phosphates, mainly detected as under-coordinated phosphorus (Figure 4) and free or-thophosphates. P3C have been reported before in melt glasses[16] and appear here during relax-ation. In the case of N25 there is also a 1% in-crease of Q^3 phosphates caused by the formation of ring structures (Figures 4 and 5).

Lower values of network connectivity are closely related to the bioactivity and increase in the solubility of the glass, but, as stated in previ-ous studies[10], the value of the NC is only associ-ated with the number of phosphates and not with the Ca^{2+}/Na^+ ratio in the PBG composition. It is therefore relevant to analyse the interactions of the cation modifiers in the surfaces.

	N25	N20	N15
Ca CN	5.05	5.37	5.22
Ca-BO	0.44	0.46	0.45
Ca-NBO	4.62	4.91	4.78
$CN_{Ca\text{-}NBO/Ca\text{-}BO}$	10.5	10.7	11.2
Na CN	4.86	4.95	4.97
Na-BO	0.89	0.92	0.97
Na-NBO	3.97	4.03	4.01
$CN_{Ca\text{-}NBO/Ca\text{-}BO}$	4.46	4.38	4.13

Table 4 Coordination numbers for the modifiers in the surface. The values are averaged over the four surfaces.

5.3 Cation coordination

Ruiz Hernandez *et al.* have analysed the coordi-nation numbers (CN) of both Ca^{2+} and Na^+ mod-ifiers in the surface region[11], as collected in Table 4. Owing to the creation of the surface from the bulk, it was found that the coordination numbers of the ions closer to the interface are lower than those found in the bulk.

Similarly to the behaviour in the bulk, $CN_{Ca\text{-}NBO/Ca\text{-}BO} > CN_{Na\text{-}NBO/Na\text{-}BO}$ for surfaces of the three compositions. Calcium has a higher

field strength than sodium and will bond to more NBOs, cross-linking more phosphates and strengthening the glass structure[10].

In order to confirm the suggestions obtained through the CN the number of chains bonded to each modifier were also computed. As already mentioned, for the bulk glasses, on average, a Ca^{2+} is bonded to 3:9 4:0 chains, while a Na^{+} is only bonded to 3:2 3:3 chains[10]. These val-ues fall in the surfaces to 2:8 3:0 chains bonded to Ca^{2+} and 2:5 2:7 chains bonded to Na^{+}, sug-gesting that a lower calcium content in the PBG will also lead to weaker structures and higher sol-ubility rates in the glass surfaces.

5.4 Discussion

The surfaces of the three compositions were frag-mented in a similar fashion. However, all the sur-faces of the compositions studied experienced an enrichment in sodium, but it is the higher Na^{+} fraction in the bulk that determined the sodium content in the surfaces. Furthermore, in N20 there are not as many Na^{+} ions exposed at the in-terface, i.e. closer to the solvent, (see concentra-tions in Table 2), as in other compositions. Pre-vious studies have shown that Na^{+} water inter-actions are potential initiators of surface degra-dation[50], whereas it is also known that a quick release of Na^{+} will favour Na^{+}/H^{+} (solvent) ex-change, leading to high alkalinity where the in-creasing amount of OH- induces the breaking of P O P bonds[49–51]. The surfaces with higher concentrations of sodium at the interface will thus dissolve more quickly. The calcium, how-ever, did not show a distinct tendency towards clustering in the studied range of compositions. The Ca^{2+} cations are responsible for strength-ening the network, cross-linking various chains through coordination to NBOs and it is in the N25 (lowest Ca^{2+} composition) surfaces, where calcium coordination numbers are lower, that the cations were bonded to fewer phosphate chains. These factors are the strongest contributors to a weaker network in the N25 surfaces and there-fore facilitators of the dissolution process. Sim-ilar to silicate glasses, the network dissolution has a direct impact on bioactivity. The dis-solved species will nucleate others, such as cal-cium phosphates, thereby encouraging, for ex-ample, apatite formation.

Small 3M rings are understood to be relevant to the long-term solubility of the glasses, since metal poly-phosphates are highly insoluble[52]. In the study by Ruiz Hernandez *et al.*[11], they are only formed at the interface z > 14 Å, with very few cations in the first coordination sphere, and at almost all times disconnected from the main phosphate network. Experimentally it is known that, once in solution, the phosphate rings are very stable[53,54], but their very low concentra-tions observed in the MD, the lack of solvent in the model employed and no other information from higher levels of theory, make it difficult to predict their impact.

6 Conclusions

In this paper, we have reviewed recent work on understanding the structure of bioactive phosphate-based glasses, and how the structure relates to the glass composition and dissolution rate. We have emphasised the role of com-puter simulation, usually molecular dynamics, in which our groups and others have played a lead-ing role, and shown that it is an excellent tech-nique for the characterisation of structural fea-tures at an atomic level. Three recent develop-ments have been important drivers of research in this field: the development of a reliable in-teratomic force field for classical simulations[9], the identification of modifier-phosphate bonding as the main structural motif controlling the dis-solution[10], and the simulation of the glass sur-face structure and properties[11]. Future work will need to make more quantitative predictions of

dissolution rate, as well as consider the effect of solvent and solvated ions and molecules on the surface structure.

References

1 J. C. Knowles, *Journal of Materials Chemistry*, 2003, **13**, 2395–2403.

2 N. J. Lakhkar, E. A. Abou Neel, V. Salih and J. C. Knowles, *J. Biomat. App.*, 2011, **25**, 877–93.

3 A. Kiani, N. J. Lakhkar, V. Salih, M. E. Smith, J. V. Hanna, R. J. Newport, D. M. Pickup and J. C. Knowles, *Phil. Trans. Roy. Soc. A*, 2012, **370**, 1352–75.

4 F. Foroutan, N. J. Walters, G. J. Owens, N. J. Mordan, H.-W. Kim, N. H. de Leeuw and J. C. Knowles, *Biomed. Mat.*, 2015, **10**, 045025.

5 M. Uo, M. Mizuno, Y. Kuboki, A. Makishima and F. Watari, *Biomaterials*, 1998, **19**, 2277– 2284.

6 T. Gilchrist, M. A. Glasby, D. M. Healy, G. Kelly, D. V. Lenihan, K. L. McDowall, I. A. Miller and L. M. Myles, *Br. J. Plast. Surg.*, 1998, **51**, 231–37.

7 S. P. Valappil, D. M. Pickup, D. L. Carroll, C. K. Hope, J. Pratten, R. J. Newport, M. E. Smith, M. Wilson and J. C. Knowles, *Antimicrob. Agents Chemother.*, 2007, **51**, 4453–61.

8 D. M. Pickup, R. J. Newport and J. C. Knowles, *J. Biomater. Appl.*, 2012, **26**, 613–22.

9 R. I. Ainsworth, D. D. Tommaso, J. K. Christie and N. H. de Leeuw, *The Journal of Chemical Physics*, 2012, **137**, 234502.

10 J. K. Christie, R. I. Ainsworth, D. Di Tommaso and N. H. de Leeuw, *The Journal of Physical Chemistry B*, 2013, **117**, 10652–10657.

11 S. E. Ruiz Hernandez, R. I. Ainsworth and N. H. de Leeuw, *J. Non-Cryst. Sols.*, 2016, **451**, 131–37.

12 D. Frenkel and B. Smit, *Understanding Molecular Simulation: From Algorithms to Applications*, Academic Press, 2001.

13 M. P. Allen and D. J. Tildesley, *Computer Sim-ulation Of Liquids*, OXford University Press, 1987.

14 K. Vollmayr, W. Kob and K. Binder, *Phys. Rev. B*, 1996, **54**, 15808.

15 A. Tilocca, *J. Chem. Phys.*, 2013, **139**, 114501.

16 D. Di Tommaso, R. I. Ainsworth, E. Tang and N. H. de Leeuw, *Journal of Materials Chemistry B*, 2013, **1**, 5054.

17 I. Ahmed, M. Lewis, I. Olsen and J. C. Knowles, *Biomaterials*, 2004, **25**, 491–499.

18 E. Tang, D. Di Tommaso and N. H. de Leeuw, *Advanced Engineering Materials*, 2010, **12**, B331–B338.

19 D. Carta, D. M. Pickup, J. C. Knowles, I. Ahmed, M. E. Smith and R. J. Newport, *Journal of Non-Crystalline Solids*, 2007, **353**, 1759–1765.

20 J.-J. Liang, R. Cygan and T. Alam, *Journal of Non-Crystalline Solids*, 2000, **263-264**, 167– 179.

21 B. Tischendorf, T. Alam, R. Cygan and J. Otaigbe, *Journal of Non-Crystalline Solids*, 2003, **316**, 261–272.

22 K. M. Wetherall, D. M. Pickup, R. J. Newport and G. Mountjoy, *Journal of Physics. Con-densed Matter: An Institute of Physics Journal*, 2009, **21**, 035109.

23 A. Tilocca, A. N. Cormack and N. H. de Leeuw, *Chemistry of Materials*, 2007, **19**, 95–103.

24 A. Tilocca, *The Journal of Chemical Physics*, 2008, **129**, 084504.

25 R. I. Ainsworth, D. D. Tommaso and N. H. de Leeuw, *The Journal of Chemical Physics*, 2011, **135**, 234513.

26 M. J. Sanders, M. Leslie and C. R. A. Catlow, *Journal of the Chemical Society, Chemical Communications*, 1984, 1271.

27 A. Tilocca, N. H. de Leeuw and A. N. Cor-

mack, *Physical Review B*, 2006, **73**, 104209.
28 D. M. Pickup, I. Ahmed, P. Guerry, J. C. Knowles, M. E. Smith and R. J. Newport, *Journal of Physics: Condensed Matter*, 2007, **19**, 415116.
29 Z. Strnad, *Biomaterials*, 1992, **13**, 317–21.
30 R. G. Hill, *J. Mater. Sci. Lett.*, 1996, **15**, 1122– 25.
31 F. Döhler, A. Mandlule, L. Van Wüllen, M. Friedrich and D. Brauer, *J. Mater. Chem. B*, 2015, **3**, 1125–34.
32 N. Lahkhar, I.-H. Lee, H.-W. Kim, V. Salih, I. Wall and J. Knowles, *Adv. Drug Deliv. Rev.*, 2013, **65**, 405–20.
33 E. Abou Neel and J. Knowles, *J. Mater. Sci.: Mater. Med.*, 2008, **19**, 377–86.
34 J. K. Christie, R. I. Ainsworth and N. H. de Leeuw, *Biomaterials*, 2014, **35**, 6164–71.
35 N. Lahkhar, E. Abou Neel, V. Salih and J. Knowles, *J. Mater. Sci.: Mater. Med.*, 2009, **20**, 1339–46.
36 J. K. Christie, A. Pedone, M. C. Menziani and A. Tilocca, *J. Phys. Chem. B*, 2011, **115**, 2038–45.
37 R. I. Ainsworth, J. K. Christie and N. H. de Leeuw, *Phys. Chem. Chem. Phys.*, 2014, **16**, 21135–43.
38 J. K. Christie, R. I. Ainsworth and N. H. de Leeuw, *J. Non-Cryst. Sols.*, 2016, **432**, 31–34.
39 J. K. Christie and N. H. de Leeuw, *J. Mater. Sci.*, 2017, **52**, 9014–22.
40 E. Berardo, M. Corno, A. N. Cormack, P. Ugliengo and A. Tilocca, *RSC Adv.*, 2014, **4**, 36425–36.
41 J. Malik and A. Tilocca, *J. Phys. Chem. B*, 2013, **117**, 14518–28.
42 A. Côté, A. N. Cormack and A. Tilocca, *J. Phys. Chem. B*, 2016, **120**, 11773–80.
43 A. Côté, A. N. Cormack and A. Tilocca, *J. Mater. Sci.*, 2017, **52**, 9006–13.
44 J. Du and A. N. Cormack, *J. Am. Ceram. Soc.*, 2005, **88**, 2532–39.
45 I. Abrahams, K. Franks, G. E. Hawkes, G. Philippou, J. C. Knowles, P. Bodart and T. Nunes, *J. Mater. Chem.*, 1997, **7**, 1573–80.
46 A. Tilocca and A. N. Cormack, *Water*, 2008, 11936–45.
47 S. Wallace, J. K. West and L. L. Hench, *J. Non-Cryst. Sols.*, 1993, **152**, 101–08.
48 N. Sahai and M. Anseau, *Biomaterials*, 2005, **26**, 5763–70.
49 A. Tilocca and A. N. Cormack, *Langmuir*, 2010, **26**, 545–51.
50 A. Tilocca and A. N. Cormack, *ACS Appl. Mater. Interfaces*, 2009, **1**, 1324–33.
51 R. Pyare, L. J. Lai, V. C. Joshi and V. K. Singh, *J. Am. Ceram. Soc.*, 1996, **79**, 1329–34.
52 D. E. C. Corbridge, *The structural chemistry of phosphorus*, Elsevier Scientific Publishing Co., 1974.
53 E. A. Abou Neel, D. M. Pickup, S. P. Valappil, R. J. Newport and J. C. Knowles, *J. Mater. Chem.*, 2009, **19**, 690–701.
54 B. C. Sales, L. A. Boatner and J. O. Ramey, *J. Non-Cryst. Sols.*, 2000, **263**, 155–66.